非粘性流のラグランジュ的性質(乱流の発生と統計法則)

AUTHOR(S):

Ohkitani, Koji

CITATION:

Ohkitani, Koji. 非粘性流のラグランジュ的性質(乱流の発生と統計法則). 数理解析研究所講究録 1992, 800: 170-184

ISSUE DATE:

1992-08

URL:

http://hdl.handle.net/2433/82836

数理解析研究所講究録
第800巻 1992年 170-184

非粘性流のラグランジュ的性質

京大数理研 大木谷耕司 (Koji Ohkitani)

Onset of energy dissipation at a finite time in high Reynolds number three-dimensional flows, which starts from a smooth initial condition, underlies Kolmogorov's theory of turbulence. This vaguely suggests a possibility of finite-time blow-up of the enstrophy, the mean square vorticity, of the Euler equations. Several numerical simulations[1,2] show a rapid increase of vorticity, however, neither presence nor absence of singularity was established[3], except for axisymmetric flows[4,5]. In this paper we propose a Lagrangian frozen-in hypothesis as a local vorticity -strain correlation in order to better explain the numerically observed behavior.

We first derive a nonlinear ordinary differential equation which governs the peak value of the vorticity and strain under the Lagrangian frozen-in hypothesis. This hypothesis is an immediate extension from the two-dimensional case,[6] the validity of the latter was examined in a recent numerical study of Euler equations.[7]

The vorticity equation for an inviscid fluid reads(summation implicit for repeated indices)

$$\frac{D\omega_i}{Dt} = S_{ij}\omega_j, \tag{1}$$

where $\frac{D}{Dt} = \frac{\partial}{\partial t} + (\boldsymbol{u}\cdot\nabla)$ denotes the Lagrangian derivative and $S_{ij} = \frac{1}{2}(\partial u_i/\partial x_j + \partial u_j/\partial x_i); i,j = 1,2,3$ the rate-of-strain tensor. Mathematically rigorous bounds[8] on the (Sobolev) norm[9] of the velocity have been obtained for flows with $\| \boldsymbol{u}(\boldsymbol{x},0) \|_s < \infty, (s \geq 3)$

as

$$\| \boldsymbol{u}(\boldsymbol{x},t) \|_s \leq \| \boldsymbol{u}(\boldsymbol{x},0) \|_s \exp(C\exp(CI_{\mathrm{BKM}}(t))), \tag{2}$$

$$\| \boldsymbol{u}(\boldsymbol{x},t) \|_s \leq \| \boldsymbol{u}(\boldsymbol{x},0) \|_s \exp(CI_{\mathrm{P}}(t)). \tag{3}$$

Here, we set $I_{\mathrm{BKM}}(t) = \int_0^t \sup|\boldsymbol{\omega}(\boldsymbol{x},t')|dt'$ and $I_{\mathrm{P}}(t) = \int_0^t \sup|S_{ij}(\boldsymbol{x},t')|dt'$ and C is a constant. These bounds implies that if a solution loses regularity at a finite time, then not only the vorticity but the strain becomes infinite simultaneously. On the other hand, a possibility for the classical solution to break down with the finite total enstrophy cannot be ruled out[2]. Though the estimates do not necessarily imply that increase in vorticity and strain occur at the same location, we can construct a phenomenological model which has such a property as a direct consequence.

Suppose that a flow starts from a smooth initial condition. The Lagrangian frozen-hypothesis means that singular structures, that is, regions with high vorticity and strain move with an inviscid fluid. We consider the evolution of a particular structure associated with a particle $\boldsymbol{a}$ or approximately its surrounding neighbors. The hypothesis can be stated more precisely as follows.

First, we suppose from the results of numerical simulation[2] that i) the vorticity aligns with the strain eigenvector;

$$S_{ij}(\boldsymbol{a},t)\omega_j(\boldsymbol{a},t) = \lambda_2(\boldsymbol{a},t)\omega_i(\boldsymbol{a},t), \tag{4}$$

associated with the second largest eigenvalue $\lambda_2(\boldsymbol{a},t) > 0$ of S_{ij}. (Three eigenvalues of S_{ij} are denoted by $\lambda_1, \lambda_2, \lambda_3$, where $\lambda_1 \geq \lambda_2 \geq \lambda_3$.) If i) is valid from $t = 0$, then we have formally $\boldsymbol{\omega}(\boldsymbol{a},t) = \boldsymbol{\omega}(\boldsymbol{a},0)\exp\int_0^t \lambda_2(\boldsymbol{a},t')dt'$ for $t > 0$, implying that rapid growth in vorticity and strain occur at the same particle.

Here we introduce two quantities A and r. One is the difference between vorticity and strain,

$$A(\boldsymbol{a},t) = \omega_i^2(\boldsymbol{a},t)/2 - S_{ij}^2(\boldsymbol{a},t). \tag{5}$$

Note that A represents a nonlocal effect[10] due to the pressure, because we have $A(\boldsymbol{a},t) = \nabla^2 p$ from $D\boldsymbol{u}/Dt = -\nabla p$. The other r specifies the ratio of the relevant eigenvalue to the strain (equivalent to assigning a ratio between two eigenvalues including λ_2)

$$r(\boldsymbol{a},t) = \lambda_2(\boldsymbol{a},t)/(S_{ij}^2(\boldsymbol{a},t))^{\frac{1}{2}}. \tag{6}$$

Because of the incompressibility condition and $\sum_{i=1}^{3} \lambda_i^2 = S_{ij}^2$, we have $|\lambda_2| \leq (S_{ij}^2)^{\frac{1}{2}}/\sqrt{6}$. In terms of r and A, the maximum vorticity $q(t) = |\boldsymbol{\omega}(\boldsymbol{a},t)|^2/2$ satisfies a nonlinear ordinary differential equation

$$\frac{dq}{dt} = 2rq\sqrt{q-A}. \tag{7}$$

Now we make two assumptions by extending the consequences of Weiss' hypothesis[6] for two-dimensional flows into three dimensions. Because strain and vorticity compete with each other while growing, it is likely that (ii) the (positive) difference A changes more slowly in time than themselves. Finally, we assume that (iii) r also varies slowly in time. This is true when λ_2 has the same asymptotic time dependence as λ_1 (or λ_3). It should be noted that without the assumption (iii) the following relations (8)-(10) hold as *inequalities* with $r = 1/\sqrt{6}$, which bound the left hand sides from above because $r(\boldsymbol{a},t) < 1/\sqrt{6}$.

We will mainly consider the simplest case where $A(\boldsymbol{a})$ and $r(\boldsymbol{a})$ are strictly time-independent. In this case, (7) is solved as

$$q(t) = \frac{A}{\sin^2\{r\sqrt{A}(t_* - t)\}}, \tag{8}$$

where t_* is a constant denoting the blowup time, constrained by $r\sqrt{A}t_* < \pi/2$ to ensure a monotonic increase of q and s. The strain $s(t) = S_{ij}(\boldsymbol{a}, t)^2$ correspondingly behaves as

$$s(t) = \frac{A}{\tan^2\{r\sqrt{A}(t_* - t)\}}. \tag{9}$$

If (7) were to hold with $A < 0$,we would have $q(t) = B/\sinh^2\{r\sqrt{B}(t_* - t)\}$, and $s(t) = B/\tanh^2\{r\sqrt{B}(t_* - t)\}$ with $B = -A$. However, this is unrealistic because of a numerical fact that vorticity is larger than strain at the point of peak vorticity (see below). As $t \to t_*$, we have

$$q(t) \approx s(t) \approx \frac{1}{r^2(t_* - t)^2}, \tag{10}$$

When $|r\sqrt{A}(t_* - t)|$ is not small, the evolution is more complicated than purely algebraic. Actually, we will show that such evolution can appear to be exponential. This provides a possible explanation as to why it is difficult to observe finite-time blowup directly.

From (8) and(9), the integrals in the estimates (2),(3) are obtained as $I_{\mathrm{BKM}}(t) = \frac{\sqrt{2}}{r}\log\frac{\tan\{r\sqrt{A}t_*/2\}}{\tan\{r\sqrt{A}(t_*-t)/2\}}$ and $I_{\mathrm{P}}(t) = \frac{1}{r}\log\frac{\sin\{r\sqrt{A}t_*\}}{\sin\{r\sqrt{A}(t_*-t)\}}$, where the frozen evolution is assumed to begin at $t = 0$. Both of these become infinity at $t = t_*$ so that if the hypothesis persists it implies the the breakdown of the solution. We must be careful in using these integrals to monitor the singularity numerically, because they grow much slowly than vorticity and strain themselves. Note that (7) includes the more intuitive (local) model[11] $D\omega/Dt = S\omega \sim \omega^2$, in the limit $A \to 0$.

Here we briefly consider how (8) works in more general cases. This can be seen by calculating $\mathrm{d}q/\mathrm{d}t$ using (8) with time-dependent r and A,

$$\frac{\mathrm{d}q}{\mathrm{d}t} = 2rq\sqrt{q - A}\left[1 + \frac{\dot{A}}{2r\sqrt{A}A}\tan\{r\sqrt{A}(t_* - t)\} - (\frac{\dot{r}}{r} + \frac{\dot{A}}{2A})(t_* - t)\right], \tag{11}$$

where the overdot denotes d/dt. When $r\sqrt{A}(t_* - t)$ is not very close to $\pi/2$ and $A(\boldsymbol{a}, t)$, $r(\boldsymbol{a}, t)$ are slowly varying; $\dot{A}/A, \dot{r}/r \ll 1$ with $t_* = O(1)$, the second and third terms in the brackets can be neglected and (8) is an approximate solution to (7). We note that precise structure of the vorticity field cannot be determined at the crude level of the present phenomenology. Furthermore, the values of r and A are expected to depend on the initial condition, even if they are nearly constant.

Now we examine the above predictions together with the underlying hypotheses by numerical simulation using a 2/3– dealiased pseudo-spectral method with 128^3 grid points. Time marching was done by the second-order Runge-Kutta method. The initial condition is a phase-randomized field whose energy spectrum $E(k)$ is 1 for $k \leq 3$ and 0 otherwise. To obtain the Lagrangian characteristics we trace 128^3 particles subject to the flow with $\boldsymbol{x}(\boldsymbol{a}, t = 0) = \boldsymbol{a}$;

$$\frac{\mathrm{d}\boldsymbol{x}(\boldsymbol{a}, t)}{\mathrm{d}t} = \boldsymbol{u}(\boldsymbol{x}(\boldsymbol{a}, t), t), \tag{12}$$

by interpolating the velocity with the second-order accurate TS13 scheme[12]. The vorticity in $\boldsymbol{a}-$ space is obtained as $\widetilde{\boldsymbol{\omega}}(\boldsymbol{a}, t) = \boldsymbol{\omega}(\boldsymbol{x}(\boldsymbol{a}, t), t)$, again using interpolation.

To check the accuracy we fit the spectrum as $E(k) \propto k^{-\alpha}\exp(-\mu k)$ in $k \geq 5$. The analyticity distance is $\mu = 9.7 \times 10^{-2}, 8.2 \times 10^{-2}, 4.9 \times 10^{-2} (\approx 128/2\pi)$ and 2.8×10^{-2} for $t = 0.5, 0.6, 0.7$ and 0.8. The computation is regarded as reliable for $t \lesssim 0.7$. The energy spectra at these times are plotted in Fig.1. The rapid fall-off at highest wavenumbers disappears at $t = 0.8$ which indicates numerical inaccuracy at this time. Indeed, contours of high vorticity regions, which are rather smooth at $t = 0.7$ (see Fig.5 below), display some numerical oscillations at $t = 0.8$ (not shown). Accuracy in $\boldsymbol{a}-$ space is firstly checked

by the equivalence of enstrophy $\boldsymbol{x}-$ and $\boldsymbol{a}-$ spaces; they differ only by $6 \times 10^{-4}, 2 \times 10^{-3}$ in relative error at $t = 0.7, 0.8$. A further check is done by the Cauchy's integral

$$\widetilde{\boldsymbol{\omega}}(\boldsymbol{a}, t) = \widetilde{\boldsymbol{\omega}}(\boldsymbol{a}, 0) \cdot \frac{\partial}{\partial \boldsymbol{a}} \boldsymbol{x}(\boldsymbol{a}, t), \tag{13}$$

at $t = 0.1$. The right hand side computed by a second-order finite difference for Δx_1 agrees with the left hand side within 1% of relative error, at 91% of grid points where $|\Delta x_1 / \Delta a_1| \leq 1$ etc. We consider this satisfactory because (13) is true only when such a difference can be regarded as a derivative.

To test hypothesis i), we plot the time evolution of the direction cosines between vorticity and the three eigenvectors of S_{ij} at the point of maximum vorticity (Fig.2). The vorticity monotonically tends to align with the second eigenvector. Actually, initially violent vortex stretching starts at the point of maximum vorticity rather than maximum strain. Thus, strong vorticity makes the nearby strain grow, not the converse.

Time evolution of $100\log q(t), 100\log s(t)$ and $q(t), s(t)$ at the point of maximum vorticity are shown in Fig.3. From the logarithmic plot, $q(t)$ appears to grow exponentially consistent with other simulations[1] and so does $s(t)$ at later times. A crucial observation is obtained in the linear plot that $q(t)$ and $s(t)$ grow with their difference approximately constant. More precisely, in $0 \leq t \leq 0.7$, it changes about 10% with respect to its mean while $q(t)$ grows by a factor of 5.8 and $s(t)$ by 31. This supports the hypothesis ii).

We show evolution of $\frac{1}{r\sqrt{A}} \mathrm{Sin}^{-1} \sqrt{\frac{A}{q}}$ by squares in Fig.4. At later times, it roughly behaves as $\propto (t_* - t)^{-1}$. This is expected from (8) for constant A and r. A least-squares fit by $(t_* - t)^{-1}$ in $0.5 \leq t \leq 0.7$ estimates $t_* \approx 1.25$. In Fig.4, we also plot evolution of r (triangles) and $\frac{1}{(t_* - t)\sqrt{A}} \mathrm{Sin}^{-1} \sqrt{\frac{A}{q}}$ (circles) with $t_* = 1.25$. A good coicidence between the

two in $t \gtrsim 0.4$ shows consistency of (8) and supports iii).

The locations of the maximum vorticity in $\boldsymbol{x}-$ space are (9,26,96),(3,26,88), (3,28,87), (5,30,86),(6,32,87),(7,33,87),(8,34,87),(8,34,85) and (7,34,84) in mesh units for $t = 0, 0.1,$ ..,0.8. In $\boldsymbol{a}-$ space they are(9,26,96),(3,23,87),(2,22,86),(2,22,86), (3,23,85),(4,24,84), (4,24,83),(4,25,82) and (3,24,83). The point moves roughly in the x_2 direction in $\boldsymbol{x}-$ space, but is almost fixed in $\boldsymbol{a}-$ space.

In Fig.5 the sectional contours of q centered on the point of maximum vorticity is plotted in $\boldsymbol{x}-$ space at $t = 0.7$. The high vorticity regions take the form of *sheets*[1,2]. The shaded high strain regions indeed occupy the same location[13] consistent with the hypothesis (ii). Examination of contours at earlier times show that x_2 is roughly normal to the sheet. In Fig.6 similar plots are made in $\boldsymbol{a}-$ space, where the high vorticity regions take the form of *blobs*. This suggests that vorticity is more localized in $\boldsymbol{a}-$ space than in $\boldsymbol{x}-$ space, consistent with Lagrangian frozen-in hypothesis.

Because of a limited resolution, the present result cannot be taken as an evidence of finite-time singularity. However, it suggests that the nonlocal effect due to the pressure makes difficult the direct observation of blowup. It may be interesting to apply the present model for axisymmetric flows which were reproted to blow up[4,5].

References

[1]M. E. Brachet, D. I. Meiron, S. A. Orszag, B. G. Nickel, R. H. Morf and U. Frisch, J. Fluid Mech., **130**, 411(1983).

[2]A. Pumir and E. Siggia, Phys. Fluids A **2**, 220(1990).

[3]For simple but unphysical blow-up solutions, see K. Ohkitani, J. Phys. Soc. Jpn. **59**, 3811(1990); **60**, 1144(1991) and references cited therein.

[4] R. Grauer and T. C. Sideris, Phys. Rev. Lett **67**, 3511(1991).

[5] A. Pumir and E. D. Siggia, Phys. Rev. Lett. **68**, 1511(1992).

[6]J. Weiss, Physica D**48**, 273(1991).

[7]K. Ohkitani, J. Phys. Soc. Jpn. **61**, 753(1992).

[8]J. T. Beale, T. Kato and A. Majda, Commun. Math. Phys. **94**, 61(1984); G. Ponce, Commun. Math. Phys. **98**, 349(1985); R. E. Caflisch, in *the Proceedings of the Workshop on Mathematical Aspects of Vortex Dynamics*, ed. by R. E. Caflish (SIAM, Philadelphia, PA, 1989), p.1; A. Majda, SIAM Review **33**, 349(1991).

[9]Defined by $\| \boldsymbol{u}(\boldsymbol{x},t) \|_s = \{ \sum_{\alpha_1+\alpha_2+\alpha_3 \le s} \int (\frac{\partial^{\alpha_1+\alpha_2+\alpha_3}}{\partial x_1^{\alpha_1} \partial x_2^{\alpha_2} \partial x_3^{\alpha_3}} \boldsymbol{u})^2 d\boldsymbol{x} \ \}^{1/2}$, where the derivatives are taken in the sense of the distributions.

[10] More generally, see B. Serrin,in *Encyclopedia of Physics*, ed. by S. Flugge (Springer,New York, 1959), p.168. For an application of this relation to a viscous flow, see S. Douady, Y. Couder, and M.E. Brachet, Phys. Rev. Lett. **67**, 983(1991).

[11]C. Bardos and U. Frisch, Lecture Notes in Mathematics **565** (Springer, 1976), p.1.

[12] P.K. Yeung and S. B. Pope, J. Comp. Phys. **79**, 373(1988).

[13] The reason why this property is invalidated at the late stage of computation in ref.2 may include instability, but is not clear.

Figure Captions

Figure 1. Energy spectra at times $t = 0.5$ (solid), 0.6(dashed), 0.7(dash-dotted) and 0.8(dash-double-dotted).

Figure 2. Time evolution of the squared direction cosines at the point of maximum vorticity between vorticity and the first (circles), second (triangles) and third(squares) eigenvector of the strain tensor. Their sum is unity.

Figure 3. Time evolution of $q(t)$(circles) and $s(t)$(squares), $100\log q(t)$(triangles) and $100\log s(t)$(plusses) at the point of maximum vorticity. Note that the difference between q and s is almost constant.

Figure 4. Time evolution of $\frac{1}{r\sqrt{A}}\mathrm{Sin}^{-1}\sqrt{\frac{A}{q}}$ (squares).The dashed line is determined by least-squares fit in $0.5 \leq t \leq 0.7$. Time evolution of r (triangles) and $\frac{1}{(t_*-t)\sqrt{A}}\mathrm{Sin}^{-1}\sqrt{\frac{A}{q}}$ (circles). Note that $r < 1/\sqrt{6} \approx 0.408$.

Figure 5. Sectional contours of vorticity centered at the maximum point of vorticity in $\boldsymbol{x}$- space $(-\pi \leq x_1 \leq \pi, 0 \leq x_2, x_3 \leq 2\pi)$ at $t = 0.7$. Regions whose strain is larger than 80% of its maximum in the plane are shaded.

Figure 6. Sectional contours of vorticity centered at the maximum point of vorticity in $\boldsymbol{a}$-space at $t = 0.7$ plotted as in Fig.5

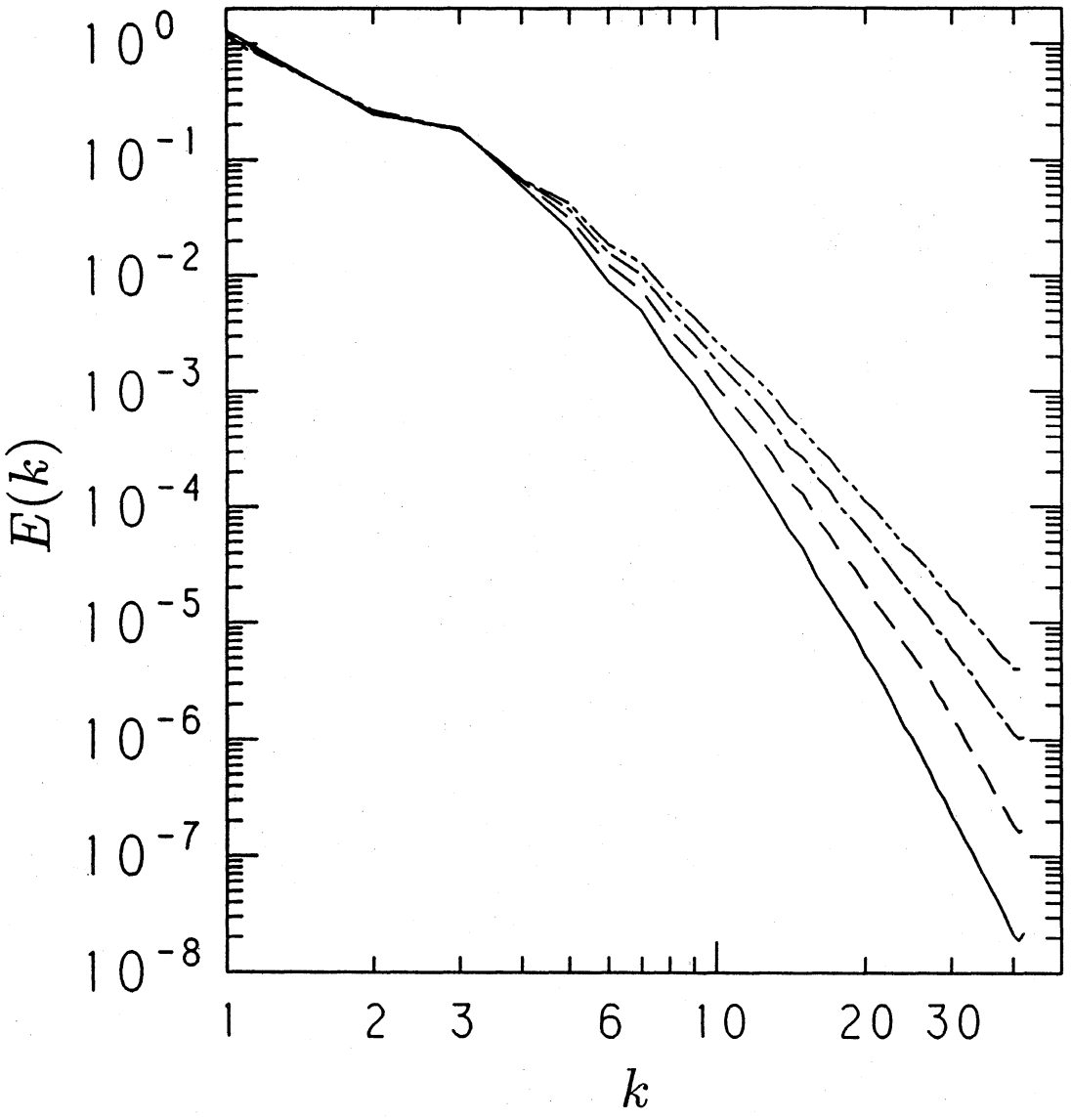

Fig. 1

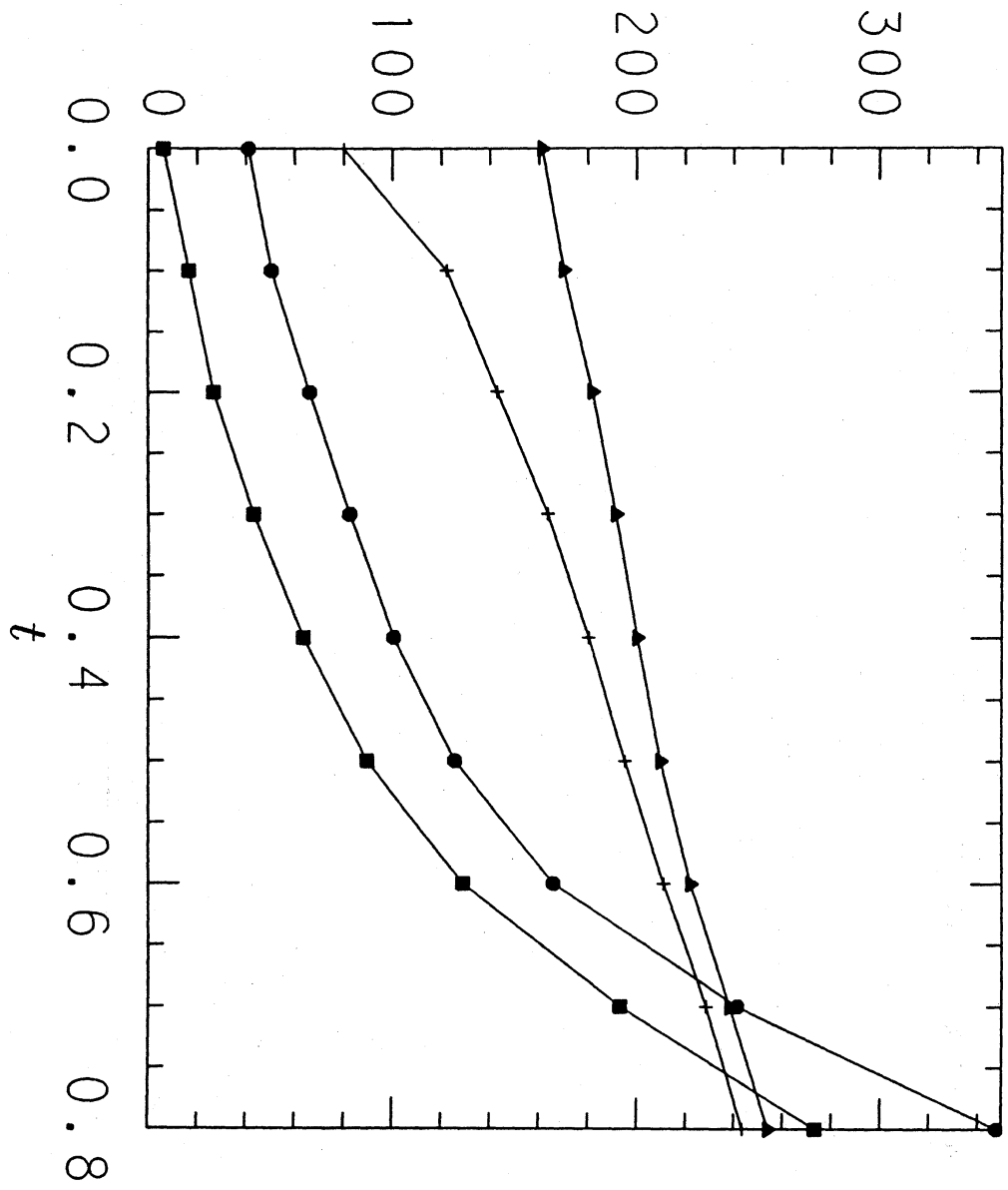

Fig. 3

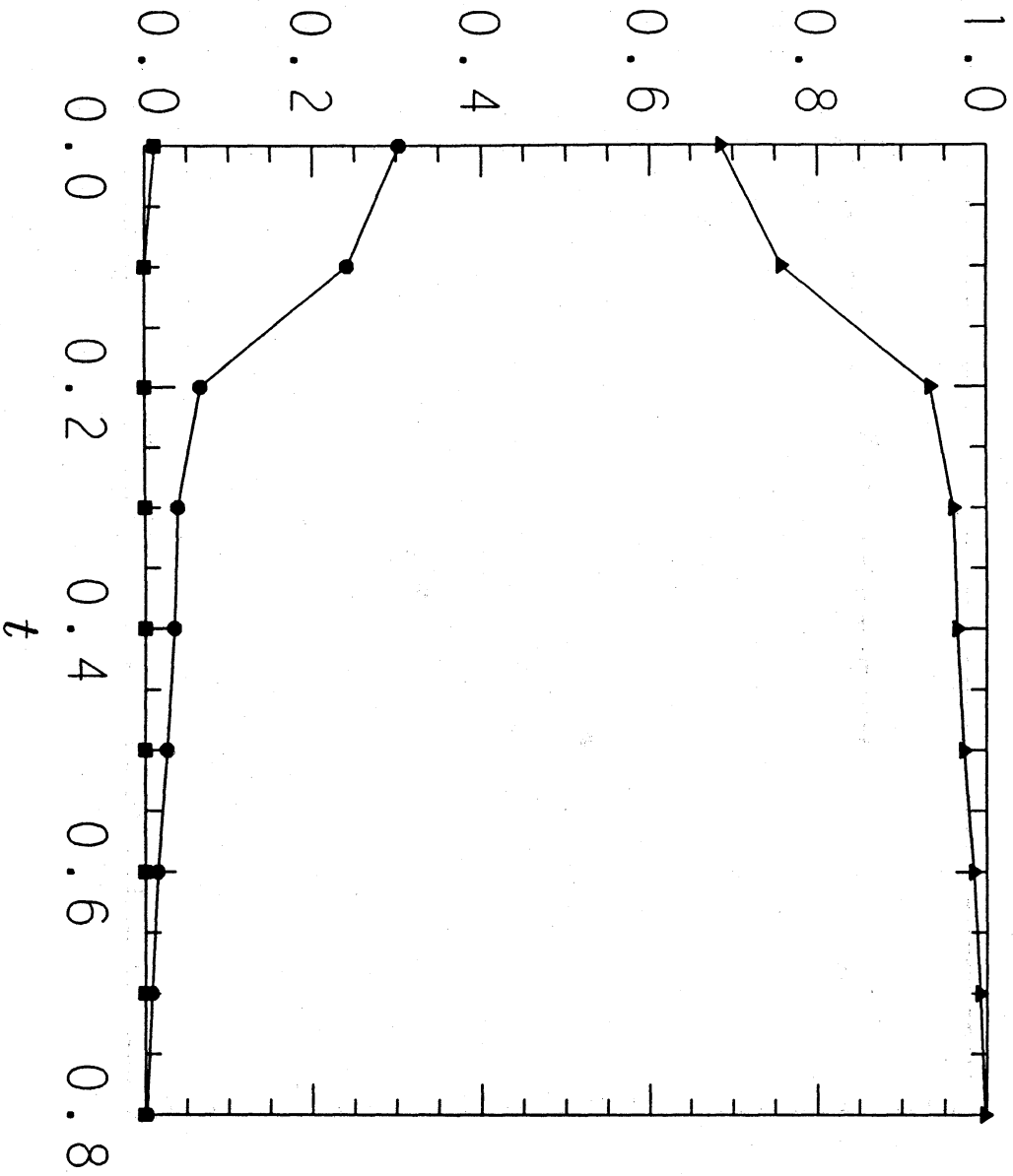

Fig 2

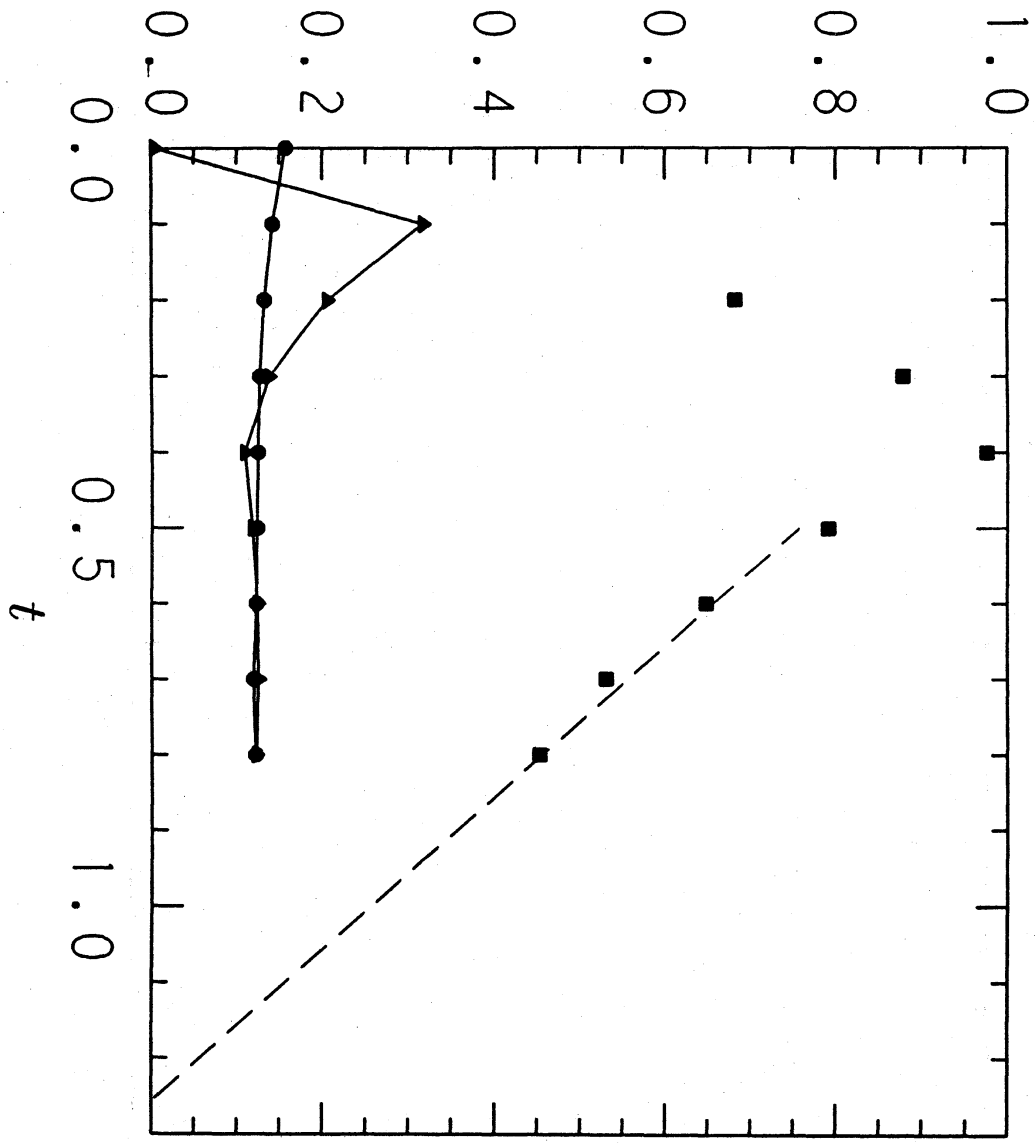

Fig. 4

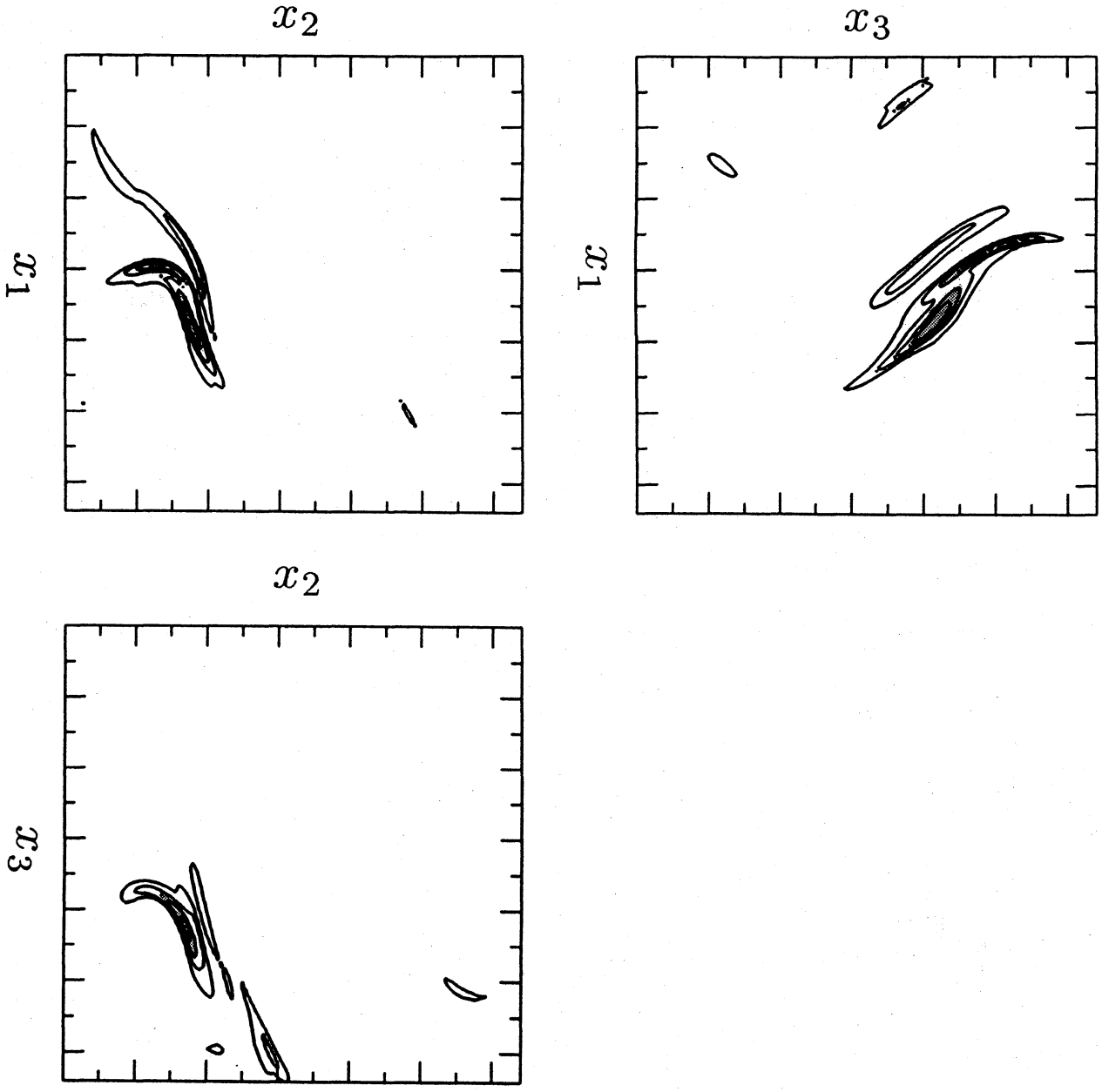

Fig.5

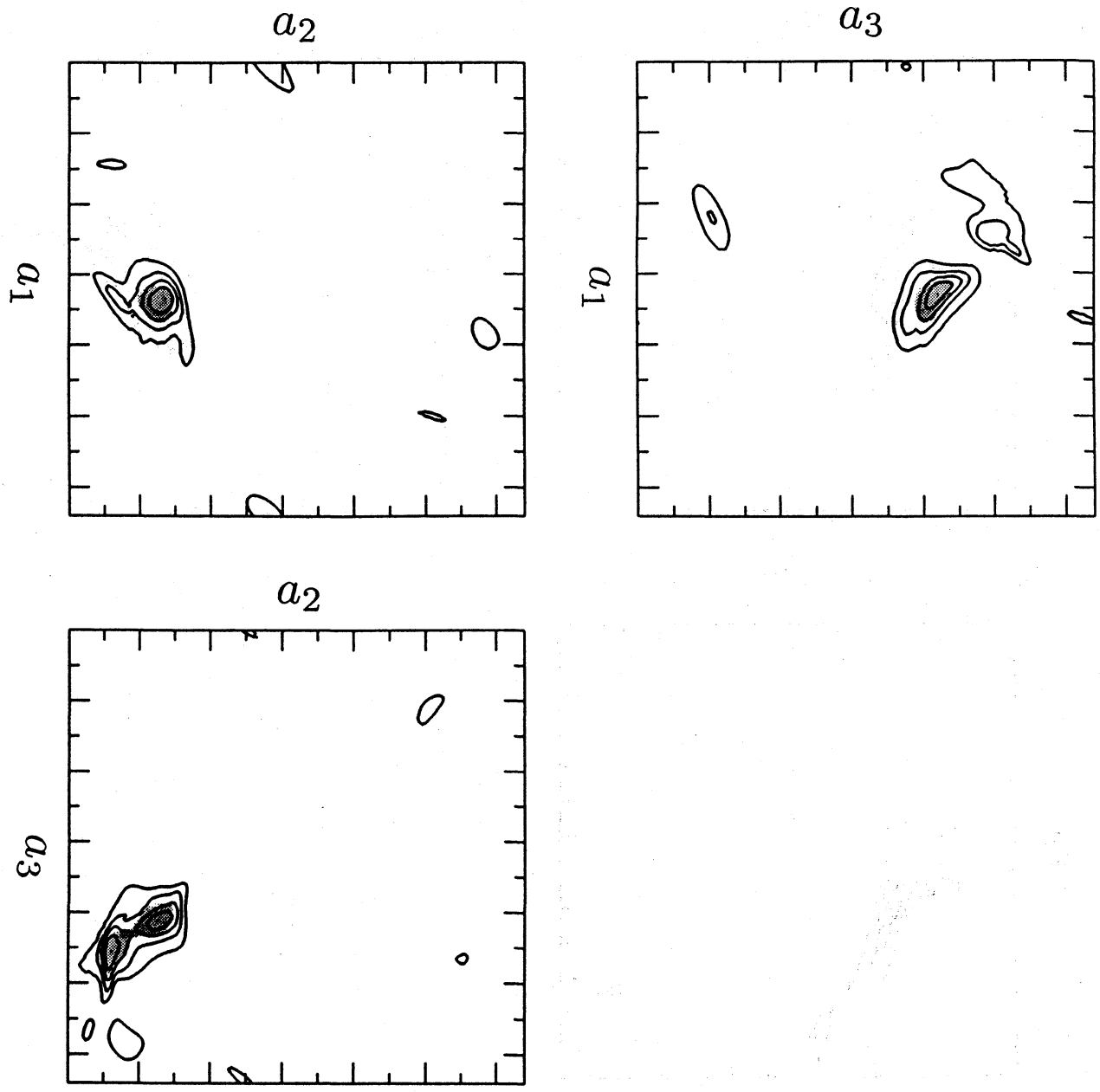

Fig. 6